Pergamon

Geochimica et Cosmochimica Acta, Vol. 66, No. 19, pp. 3431–3439, 2002
Copyright © 2002 Elsevier Science Ltd
Printed in the USA. All rights reserved
0016-7037/02 $22.00 + .00

PII S0016-7037(02)00943-2

Phase equilibria of the system methane–ethane from temperature scaling Gibbs Ensemble Monte Carlo simulation

ZHIGANG ZHANG[1,2] and ZHENHAO DUAN[1,3,*]

[1]Chinese Academy of Sciences, Institute of Geology and Geophysics, Beijing, 100029, China
[2]Faculty of Earth Resources, China University of Geosciences, Wuhan, 430074, China
[3]Department of Chemistry, 0340, University of California, San Diego, La Jolla, CA 92129, USA

(*Received November* 8, 2001; *accepted in revised form April* 30, 2002)

Abstract—A new technique of temperature scaling method combined with the conventional Gibbs Ensemble Monte Carlo simulation was used to study liquid–vapor phase equilibria of the methane–ethane (CH_4-C_2H_6) system. With this efficient method, a new set of united-atom Lennard-Jones potential parameters for pure C_2H_6 was found to be more accurate than those of previous models in the prediction of phase equilibria. Using the optimized potentials for liquid simulations (OPLS) potential for CH_4 and the potential of this study for C_2H_6, together with a simple mixing rule, we simulated the equilibrium compositions and densities of the CH_4-C_2H_6 mixtures with accuracy close to experiments. The simulated data are supplements to experiments, and may cover a larger temperature–pressure–composition space than experiments. Compared with some well-established equations of state such as Peng-Robinson equation of state (PR-EQS), the simulated results are found to be closer to experiments, at least in some temperature and pressure ranges. *Copyright © 2002 Elsevier Science Ltd*

1. INTRODUCTION

Phase separation is one of the most important mechanisms controlling many geochemical processes associated with the chemistry and thermodynamic behavior of liquid and vapor, such as the evolution of geothermal fluids (Nicholson, 1993), the transportation and deposition of minerals (Seward and Barnes, 1997), the formation and fractionating of magma (Litvinovsky, 1993), the trapping of fluid inclusions (Roedder, 1984; Bodnar and Sterner, 1987), the formation of basin fluids (Goldstein and Reynolds, 1994), and the cryogenic processing of natural gas (Al-Sahhaf et al., 1983). The knowledge of phase equilibrium is usually obtained from experimental observation. However, experimental data available are generally discrete and limited because of special requirements of laboratory conditions and the limited time or financing of the experimenters. To calculate thermodynamic properties under arbitrary thermodynamic conditions, empirical or semitheoretical models, e.g., equation of state (EOS), are used to interpolate or extrapolate data from experiments. Some well-established EOS such as the well-known Peng-Robinson EOS (Peng and Robinson, 1976), the EOS of Anderko and Pitzer (1993), and the EOS of Duan et al. (1992, 1996, 2000) can reproduce data with good accuracy in special systems and conditions. However, most of these models depend too much on a range of experimental data to evaluate the parameters.

A promising approach to study phase equilibrium is computer simulation based on molecular modeling. This approach can in principle predict vapor–liquid phase equilibrium (VLE) of a fluid system under any thermodynamic conditions, which is a remarkable advantage over the empirical or semiempirical models. Recently great progress of simulation has been made. Many novel algorithms have been proposed, such as the NPT + test particle method (Kriebel et al., 1995; Vrabec and Fischer, 1995), the Gibbs-Duhem integration method (Kofke, 1993a, b), and Histogram Reweighting Grand Canonical Monte Carlo (Panagiotopoulos et al., 1998; Potoff and Panagiotopoulos, 1998). However, the prediction of phase transitions is not simple because phase transitions are actually collective phenomena that often occur over time and length scales that are not directly accessible by molecular dynamics or simple constant-volume Monte Carlo simulations (Panagiotopoulos, 2000). The Gibbs Ensemble Monte Carlo method (GEMC) (Panagiotopoulos, 1987; Panagiotopoulos et al., 1988) presents a simple way to overcome this bottleneck and is widely used in the simulation of phase behaviors of different systems.

The major factor impacting the accuracy of the predicted thermodynamic properties by molecular-level simulations is the selection of a set of appropriate parameters of molecular interaction potentials. This inevitably involves a large number of simulation and fitting with the experimental data and is time-consuming. The scaling method is found to be of significant efficiency in this process. The basic idea of this method is to extract useful information for different thermodynamic conditions in a single simulation with non-Boltzmann sampling, which is based on the work of Valleau (1993) and was later extended to the Gibbs ensemble by Kiyohara et al. (1996).

The purpose of this paper was to study the thermodynamic properties of a relatively simple system using conventional GEMC and Temperature Scaling Gibbs Ensemble Monte Carlo (TSGE). Because TSGE can yield VLE for different temperatures in a single simulation, it is used to simulate the phase coexistence of pure system and optimize the potential parameters in this study. The GEMC was mainly adopted to study the isothermal properties of the mixture system. The system methane–ethane (CH_4-C_2H_6) was chosen for several reasons. First, a substantial amount of experimental data is available for each component and their mixtures. It is convenient to optimize the

* Author to whom correspondence should be addressed (duanzhenhao@yahoo.com).

potential parameters and make a comprehensive comparison between the simulated results and experiments. Second, as CH_4 and C_2H_6 are the most important hydrocarbons of natural gas, knowledge of their equilibrium properties is indispensable for the low-temperature processing of natural gas. Third, the two species are of considerable interest in the study of fluid-phase equilibrium and have been extensively investigated by experimental scientists.

In the next section, the simulation methods are briefly introduced. The following section presents the simulation details. In the subsequent section, the results are discussed and compared with experimental data and those from other models. Finally, some conclusions are drawn.

2. SIMULATION METHODS

Both of the simulation methods used in our study are described in detail elsewhere (Kiyohara et al., 1996; Panagiotopoulos, 1987; Panagiotopoulos et al., 1988); we summarize only the main points.

2.1. Conventional Gibbs Ensemble Monte Carlo

The Gibbs ensemble method involves setting up two simulation "boxes" (I and II), which are allowed to exchange volumes and particles and stand for two phases of the system. To simulate the equilibrium of the whole system, there are three kinds of moves in a Monte Carlo (MC) step (cycle): (1) random molecule displacements within each box to ensure equilibration within each region; (2) changes in the volumes of the two regions that result in the equality of the average pressures; and (3) random transfers of molecules between regions that result in the equality of the chemical potential of each component in the two regions.

If the coordinates of particles of the system are written as r^N, the sampling distribution of Gibbs ensemble (constant NVT version) is given by:

$$\psi(r^N) = \frac{V_I^{N_I} V_{II}^{N_{II}}}{N_I! N_{II}!} \exp(-\beta E^I - \beta E^{II}) \tag{1}$$

where E is the configurational energy, β is the reciprocal temperature ($\beta = 1/k_B T$, where k_B is Boltzmann's constant), and V_I and V_{II} are the volumes of each box.

During the simulation, the conventional Metropolis method is used (Allen and Tildesley, 1989). So the acceptance probability for either MC move from configuration j to $j+1$ is expressed as $\min(1, P_{j\to j+1})$, where

$$P_{j\to j+1} = \frac{\psi(r_{j+1}^N)}{\psi(r_j^N)} \tag{2}$$

The constant pressure version (NPT) GEMC is only different with the sampling distribution, which has the following form:

$$\psi(r^N) = \frac{V_I^{N_I} V_{II}^{N_{II}}}{\sum_\alpha N_{I\alpha}! N_{II\alpha}!} \exp(-\beta E^I - \beta E^{II} - \beta P V_I - \beta P V_{II}) \tag{3}$$

where P is the imposed system pressure, and $N_{I\alpha}$ is the number of molecules of species α in region I. V_I and V_{II} are independent in this case.

2.2. Temperature Scaling Gibbs Ensemble Monte Carlo

In conventional GEMC, the thermodynamic average of any property X at β_i is

$$\langle X \rangle_{\beta_i} = \frac{\int X(r^N)\psi(r^N;\, \beta_i) dr^N}{\int \psi(r^N;\, \beta_i) dr^N} \tag{4}$$

When a non-Boltzmann sampling distribution $\pi(r^N)$ is introduced, the average is determined from

$$\langle X \rangle_{\beta_i} = \frac{\int \pi(r^N) X(r^N) \dfrac{\psi(r^N;\, \beta_i)}{\pi(r^N)} dr^N}{\int \pi(r^N) \dfrac{\psi(r^N;\, \beta_i)}{\pi(r^N)} dr^N} = \frac{\left\langle X(r^N) \dfrac{\psi(r^N;\beta_i)}{\pi(r^N)} \right\rangle_{\pi(r^N)}}{\left\langle \dfrac{\psi(r^N;\beta_i)}{\pi(r^N)} \right\rangle_{\pi(r^N)}} \tag{5}$$

where the $\langle\ \rangle_{\pi(r^N)}$ brackets above indicate an average overall configurations sampled with distribution $\pi(r^N)$.

$\pi(r^N)$ is selected to be a linear combination of the conventional GEMC sampling distributions (Valleau, 1993), that is

$$\pi(r^N) = \sum_i W_{\beta_i} \psi(r^N;\, \beta_i) \tag{6}$$

Metropolis sampling algorithm with the same three Monte Carlo moves as GEMC is also used in TSGE. The acceptance probability for either MC move in TSGE from configuration j to $j+1$ is:

$$P_{j\to j+1} = \min\left(1, \frac{\pi(r_{j+1}^N)}{\pi(r_j^N)}\right) \tag{7}$$

As $\pi(r^N)$ should sample configurations relevant to all the configurations with equal frequency, the weights of thermodynamic states β_i and β_j should satisfy the following equation:

$$\frac{W_{\beta_j}}{W_{\beta_i}} = \frac{\left\langle \dfrac{\psi(r^N;\, \beta_i)}{\pi(r^N)} \right\rangle_{\pi(r^N)}}{\left\langle \dfrac{\psi(r^N;\, \beta_j)}{\pi(r^N)} \right\rangle_{\pi(r^N)}} \tag{8}$$

Eqns. 6 and 8 suggest that to get an appropriate set of weights, a process of iteration can be carried out, which will be introduced in detail in the next section.

Once the weights of Eqn. 6 have been determined, a propagation of the Markov chain is followed, which is the same as conventional GEMC except for the calculation of the sampling distribution. At the end of each simulation, the equilibrium density or composition can be calculated by Eqn. 5.

Table 1. Parameters of different potential models.

Interaction Unit	Fischer			OPLS			TraPPE			This study		
	ϵ/k_B(K)	σ(Å)	L	ϵ/k_B(K)	σ(Å)	L	ϵ/k_B(K)	σ(Å)	L	ϵ/k_B(K)	σ(Å)	L
CH_4	149.92	3.7327	—	147.9	3.73	—	148	3.73	—	147.9	3.73	—
CH_3 (C_2H_6)	139.81	3.512	0.67	104.1	3.775	0.4053	98	3.75	0.4107	98.59	3.747	0.4107

3. SIMULATION DETAILS

3.1. Potential Models

The Lennard-Jones (LJ) 12-6 potential was adopted in this study because of its simplicity and predictability for pure systems and for supercritical mixtures. The potential has the form:

$$u(r_{ij}) = 4\epsilon_{ij}\left[\left(\frac{\sigma_{ij}}{r_{ij}}\right)^{12} - \left(\frac{\sigma_{ij}}{r_{ij}}\right)^{6}\right], \tag{9}$$

where u is the potential energy between units (molecules or pseudoatoms) i and j, and r_{ij}, ϵ_{ij}, σ_{ij} are the separation, energy, and size parameter, respectively.

To describe the intermolecular interactions, we used different approaches for CH_4 and C_2H_6 molecules. The CH_4 molecule was approximated as a united atom with only one LJ term at the center of the carbon atom. This approach is not appropriate for the C_2H_6 molecule, which is instead modeled as a two-center molecule with a special elongation. The intermolecular interaction unit is the methyl group (CH_3-). So the potential between two C_2H_6 molecules can be calculated by

$$u_{ij} = \sum_{\alpha,\beta=1}^{2} u(r_{i\alpha j\beta}) \tag{10}$$

where α is the identity (1 or 2) of the interaction units in molecule i and β is that of another molecule j.

In this study, two methyl groups in a C_2H_6 molecule were connected by a bond with a fixed length (i.e., without fluctuation), so the intramolecular potential within a C_2H_6 molecule could be omitted.

For binary mixture parameters, the Lorentz-Berthelot combining rule was used:

$$\epsilon_{ij} = k_{1,ij}\sqrt{\epsilon_i\epsilon_j} \tag{11}$$

$$\sigma_{ij} = k_{2,ij}(\sigma_i + \sigma_j)/2 \tag{12}$$

$k_{1,ij}$ and $k_{2,ij}$ are the mixing coefficients for the combining rule.

As described above, there are two LJ parameters ϵ_{ij}, σ_{ij} and an additional parameter, bond length, for C_2H_6. The simulation results are sensitive to the selection of these parameters. A number of parameters have been published by earlier workers, e.g., those by Fischer et al. (1984), the popular OPLS potential model by Jorgensen et al. (1984), and TraPPE (transferable potentials for phase equilibria) force field by Martin and Siepmann (1998).

As shown in Table 1, we adopted OPLS for CH_4 in this study, because our computer program with the OPLS parameters of CH_4 could generate sufficiently accurate results. Among the previous models for C_2H_6, TraPPE (Martin and Siepmann, 1998) generally yields the most accurate results, but it cannot yield saturated vapor densities with sufficient accuracy. Therefore, we tried to improve the ability of prediction for vapor-saturated densities while maintaining its excellent predictability for liquid densities in this study. In principle, we must perform a lot of simulations and search over the parameter space to look for a better fit to the experimental data. For the sake of efficiency, our search started from the model parameters of TraPPE.

As described in the paper of Jorgensen et al. (1984), for a two-center molecule there is some compensation relation between σ and bond length. Following the method adopted by Fischer et al. (1984), we fixed the ratio L, $L = l_{bond}/\sigma$. In this study L was selected to be that of TraPPE (0.4107).

We performed simulations with parameters of TraPPE using the TSGE method and obtained the equilibrium liquid and vapor densities of C_2H_6, some of which are listed in Table 2. We reduced these densities and temperatures with parameters of TraPPE as:

$$T^* = k_B T/\epsilon \tag{13}$$

$$\rho^* = \rho\sigma^3 \tag{14}$$

At the same time, we calculated the simulated reduced critical properties: $T_c^* = 3.097$, $\rho_c^* = 0.2181$. The experimental data were then reduced with new values of ϵ and σ according to Eqns. 13 and 14. $\epsilon = 98.59$ K, $\sigma = 3.747$ Å are obtained by minimizing the deviation between the reduced experimental data and the fitted curve of the simulation points (including subcritical densities and critical point). So the new bond length is, $l_{bond} = L * \sigma = 1.539$Å.

Table 2. Part of simulation results of C_2H_6 with the parameters of TraPPE.

T(K)	Density of liquid (kg/m^3)		Density of vapor (kg/m^3)	
	Exp.[a]	TraPPE	Exp.[a]	TraPPE
293	339.93	335.4	85.922	90.579
273	400.92	393.6	46.077	52.108
258	432.94	423.1	29.923	35.645
238	468.36	460.6	16.434	22.682
208	513.12	506.8	5.782	8.216
168	564.31	560.3	0.822	1.094

[a] Smoothed experimental data of Friend et al. (1991).

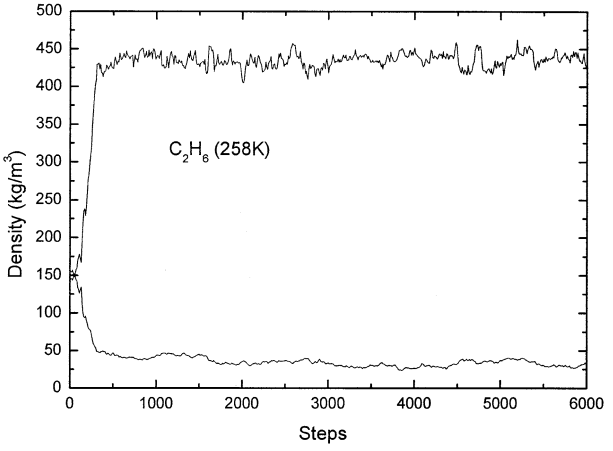

Fig. 1. The density change during a GEMC simulation for C_2H_6 at 258 K.

3.2. Gibbs Ensemble Simulation

At first, the initial conditions for the two simulation boxes were set up independently. The coordinates of the CH_4 and C_2H_6 particles were initiated from the face-centered cubic lattice structure. Some (about twice as many as total number of molecules) random exchanges of initial positions of different components were helpful in reducing equilibrium time. The orientations of C_2H_6 molecules were initially set to be parallel to the z-axis of the Cartesian coordinate system. The total molecule number of the two boxes was 512 in our simulations. There was little difference in the results if we increase the number to 1000.

In the following process, three MC moves (mentioned above) were used to sample phase space, and there were two kinds of molecule displacement for C_2H_6: translations and rotations. We used the method suggested by Jansoone (1974) to change the orientation of a C_2H_6 molecule. Each Monte Carlo step (cycle) constituted by these MC moves consists of 3 to 5 times the total number of molecules of attempted displacements (with equal probability of translation and rotation), 1 to 2 attempted volume changes, and 50 to 200 attempted interchanges. The maximum displacement of translations, rotations, and volume moves was adjusted at the end of every 10 steps to yield acceptance rates of 50%. Whether or not the system has reached equilibrium is judged by monitoring the densities (or configuration energy) of the two phases vs. simulation steps (e.g., Fig. 1). If the densities (or configuration energy) fluctuate around certain values, the system is considered as reaching equilibrium. The total number of steps in a simulation was usually 6000 to 8000, with ~2000 to 3000 cycles of preequilibrium and 4000 to 5000 steps of data collection. However, the successful interchanges decrease dramatically with lowering temperatures. Therefore, more running cycles were needed for low temperatures.

The cutoff distance for intermolecular interactions was set to be half of the box length. If the distance between any two interaction units was less than $0.8 * \sigma$, the configuration would be immediately rejected. The long-range corrections U_{LRC} and P_{LRC} were added to the configuration energy and internal pressure (Allen and Tildesley, 1989):

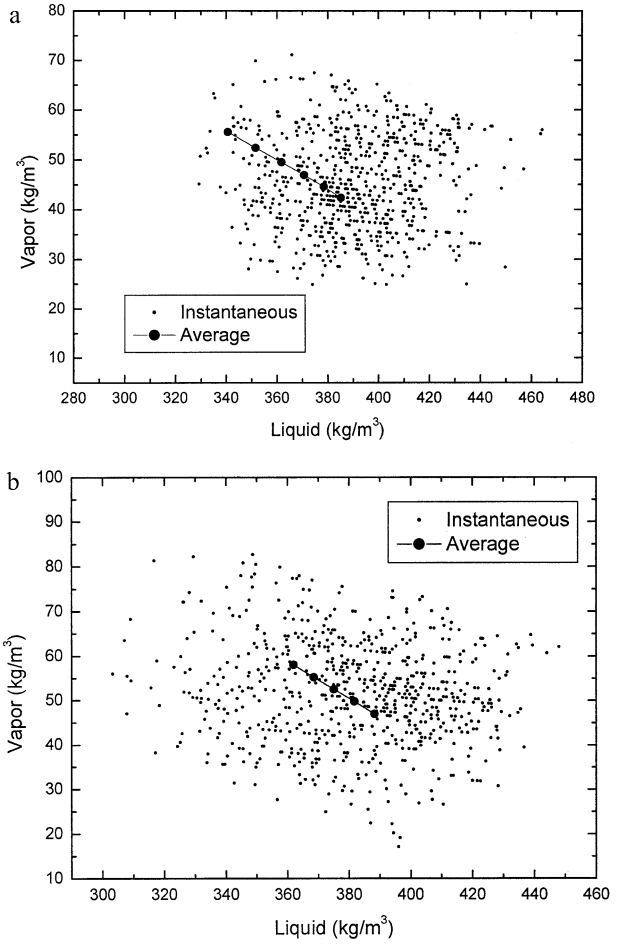

Fig. 2. An example of sampling in the course of the exploratory simulations of weights in a TSGE simulation (in the temperature range from 270 K to 280 K): (a) poor sampling; (b) good sampling.

$$U_{LRC} = \frac{16\pi}{V}\sum_{i}^{N}\sum_{i<j}^{N} n_i n_j \epsilon_{ij}\sigma_{ij}^3\left[\frac{1}{9}\left(\frac{\sigma_{ij}}{r_{cut}}\right)^9 - \frac{1}{3}\left(\frac{\sigma_{ij}}{r_{cut}}\right)^3\right] \quad (15)$$

$$P_{LRC} = \frac{32\pi}{V^2}\sum_{i}^{N}\sum_{i<j}^{N} n_i n_j \epsilon_{ij}\sigma_{ij}^3\left[\frac{2}{9}\left(\frac{\sigma_{ij}}{r_{cut}}\right)^9 - \frac{1}{3}\left(\frac{\sigma_{ij}}{r_{cut}}\right)^3\right] \quad (16)$$

where i and j are identities of two interacting molecules, N is the total number of molecules in the simulation box, so Eqns. 15 and 16 are the summations of all pair-interactions in the box. V is the volume of the box, r_{cut} is the cutoff distance, n is the number of interaction centers of a specific molecule. For CH_4, $n = 1$, whereas for C_2H_6, $n = 2$.

3.3. Temperature Scaling Gibbs Ensemble Simulation

In TSGE simulations, it is crucial to get an appropriate set of weights to achieve good sampling. So an iteration process of Eqns. 6 and 8 was adopted. First, all of the sampling weights were set to be 1.0. Then a short simulation (4000 to 6000 steps) with the sampling distribution derived from Eqn. 6 was performed. Instantaneous (every 10 steps or so) and average values

of density in the two phases were plotted in one graph. From this graph, we can tell whether or not the thermodynamic states of the whole temperature range (e.g., 270 to 280 K in Fig. 2) have been sampled well. If the small dots (which stand for instantaneous density values) are distributed uniformly around the average values of the whole temperature range, the average values are calculated from a good sampling. If not, the thermodynamic states under some temperatures are poorly sampled and thus the calculated average values are unreliable. In this step, usually the states of lower temperatures were sampled well whereas those of high temperatures were not, as shown in Figure 2a. Then the weights of those thermodynamic states that were well sampled were changed with Eqn. 8. In the next simulation, the new weights were adopted and this process was repeated with increased number of steps (5000 to 8000 steps) to sample a wider range of states. This process continues until a set of weights of Eqn. 6 is determined that sufficiently explores all relevant configurations, as illustrated in Figure 2b.

In principle, we should iterate the weights many times until they are convergent to obtain a perfectly uniform sampling. However, from Eqn. 5, the average value of a thermodynamic property X is irrelevant to the sampling distribution in theory. In practice, a sampling that has visited each of the thermodynamic states with sufficient frequency is enough, and strict uniformity of sampling is quite unnecessary. Usually, after all of the thermodynamic states are sampled with adequate frequency, 2 to 3 times more iterations are enough to get an appropriate set of weights. If the temperature range is wide, more iterations are needed. In this case, it is useful to divide the whole range into several subranges.

In the process of searching for the weights of $\pi(r^N)$, it is useful to discuss the relationship between weights W_{β_i} and the potential (excess) parts of Helmholtz free energy $A^{ex}_{\beta_i}$ because in canonical ensemble,

$$\frac{\exp(\beta_j A^{ex}_{\beta_j})}{\exp(\beta_i A^{ex}_{\beta_i})} = \frac{\int dr^N \psi(r^N;\beta_i)}{\int dr^N \psi(r^N;\beta_j} = \frac{\int dr^N \pi(r^N)\,\dfrac{\psi(r^N;\beta_i)}{\pi(r^N)}}{\int dr^N \pi(r^N)\,\dfrac{\psi(r^N;\beta_j)}{\pi(r^N)}}$$

$$= \frac{\left\langle \dfrac{\psi(r^N;\beta_i)}{\pi(r^N)} \right\rangle_{\pi(r^N)}}{\left\langle \dfrac{\psi(r^N;\beta_j)}{\pi(r^N)} \right\rangle_{\pi(r^N)}} \qquad (17)$$

From Eqns. 17 and 8, we get

$$W_{\beta_i} = C \exp(\beta_i A^{ex}_{\beta_i}) \qquad (18)$$

where C is a constant.

As $A^{ex}_{\beta_i}$ is usually a smooth function of temperature, so in practice we can fit the weights for the well-sampled regions with the form:

$$W_{\beta_i} = C \exp(f(\beta_i)) \qquad (19)$$

where $f(\beta_i)$ is usually a polynomial function of temperature. Eqn. 19 is also valid in other ensembles. With this function, we can predict the weights for the regions not sampled well. In this way the exploratory simulations for weights can be significantly shortened.

Table 3. An example of Temperature Scaling Gibbs Ensemble simulation.

Temperature (K)	Weights	Densities: Liquid (kg/m^3)	Densities: Vapor (kg/m^3)
280.0	28037606	371.97	58.04
278.0	501668	378.51	55.22
276.0	7562	385.09	52.50
274.0	95	391.73	49.80
272.0	1	398.30	46.96

In this study we tried to cover most of the liquid–vapor phase transition temperature ranges of pure systems and divided these ranges into 4 to 6 subranges. In the vicinity of critical points, the subtemperature ranges of TSGE were narrower, usually 10 to 15 K.

Table 3 presents an example of TSGE simulation of C_2H_6 in a region of 270 to 280 K. As discussed above, the logarithms of weights $\ln(W_{\beta_i})$ vs. temperature differences $\Delta T = T - T_{\min}$ were plotted in Figure 3. Actually, we could find a good linear relationship between these two quantities, with the form:

$$\ln(W_{\beta_i}) = -0.0222(\Delta T)^2 + 2.3211\Delta T + 0.0003 \qquad (20)$$

With this set of weights, in the following process of ~9000 steps of propagating the Markov chain, instantaneous values inside the brackets of numerator and denominator of Eqn. 5 for the densities of two phases were summed up. With Eqn. 5 the densities of two phases under different temperatures could be calculated, which were also listed in Table 3. The simulated results are consistent with the corresponding results of GEMC.

The TSGE method shows its advantage of significant efficiency over conventional GEMC when a large number of thermodynamic states at different temperatures are interested. When a few points of different temperatures or isotherm behaviors are interested, GEMC simulation would be preferable.

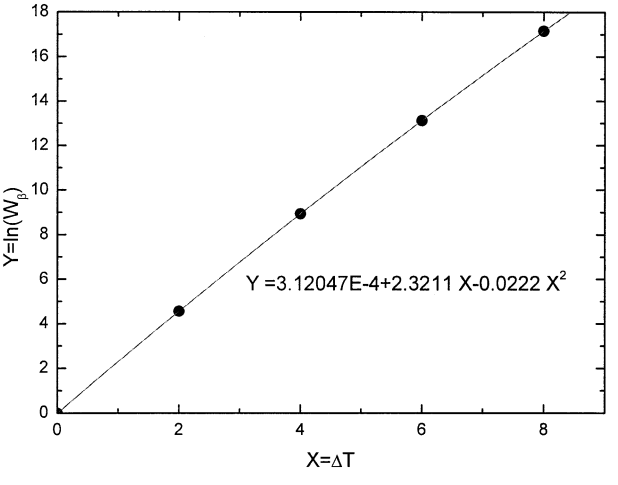

Fig. 3. The relationship between weights and temperature intervals.

Table 4. Simulated CH_4 saturated densities and latent heats vs. experimental data.

	Density of liquid (kg/m^3)		Density of vapor (kg/m^3)		Latent heat (KJ/mol)	
T(K)	Exp.[a]	Simulated	Exp.[a]	Simulated	Exp.[a]	Simulated
180	276.23	279.24(5.93)[b]	61.375	57.944(4.182)	3.9607	4.189(.2043)
165	324.10	326.27(3.97)	31.448	31.344(2.417)	5.5847	5.647(.0483)
150	357.90	355.55(3.59)	16.328	17.310(1.339)	6.6190	6.558(.0581)
140	376.87	372.75(2.89)	10.152	9.427(.443)	7.1413	7.071(.0466)
120	409.90	407.69(2.469)	3.262	3.390(.152)	7.9350	7.930(.0597)

[a] Smoothed experimental data by an equation of state of Setzmann and Wagner (1991).
[b] The numbers in the parentheses are the uncertainties in the simulation. For example, 3.390(.152) means 3.390 ± 0.152.

So in this study, we used TSGE to study the phase behavior of pure systems under a number of subcritical temperatures, whereas GEMC was adopted to simulate the isotherm phase behavior of mixtures.

4. RESULTS AND DISCUSSION

4.1. Pure Systems

The liquid–vapor equilibrium densities and the latent heats of CH_4 simulated in this study are partially listed in Table 4. It can be seen that the experimental data (Setzmann and Wagner, 1991) are approximately within the uncertainty of the simulation results. As for the saturated liquid densities, the largest error is less than 1.1%, which is a remarkable accuracy. For saturated vapor densities the relative errors are a little larger, the maximum of which is ~7.1%. The average deviation of simulated latent heat from experiments is less than 1.2% except in the vicinity region of critical point, where the largest relative error was ~5.8%. The comparisons are more evident in Figure 4.

Figure 5 shows the simulated and experimental coexistence line of C_2H_6. The simulations have virtually generated the same results as experiments (Friend et al., 1991). To draw a comparison between the results obtained with different models, the simulated equilibrium liquid densities, vapor densities, and latent heats are presented in Figures 6, 7, and 8, respectively. The simulations of this study are found to have the same accuracy with TraPPE for liquid, but are more precise for vapor and latent heat. The simulated results with Fischer et al. (1984) are in good agreement with experiments only in the region below 240 K and OPLS below 210 K.

With the simulated results, we can calculate the critical properties of CH_4 and C_2H_6 by fitting the simulated data with the following equations:

$$\rho_l - \rho_v = B(T - T_c)^\beta \tag{21}$$

$$\frac{\rho_l + \rho_v}{2} = \rho_c + A(T - T_c) \tag{22}$$

where ρ_l and ρ_v are the densities of saturated liquid and vapor, respectively. A and B are fitting constants.

In this research, β was selected to be 0.33. It is usually reasonable to select any value between 0.32 and 0.34 for nonionic fluids.

The critical points of different models listed in Table 5 are all calculated with our own program, and the results with other models are found to agree with the original publications. Obviously, the critical properties of CH_4 using OPLS and C_2H_6

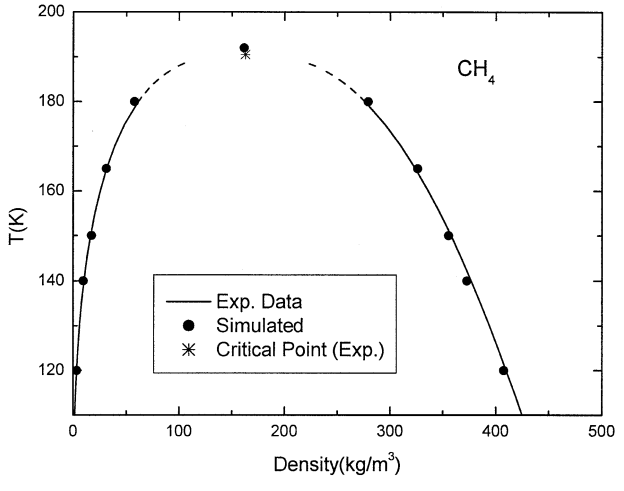

Fig. 4. Comparison of experimental liquid–vapor phase equilibria of CH_4 with the simulated results of this study. The solid line represents smoothed experimental data from Setzmann and Wagner (1991), and the dashed line is the extrapolation from experiment.

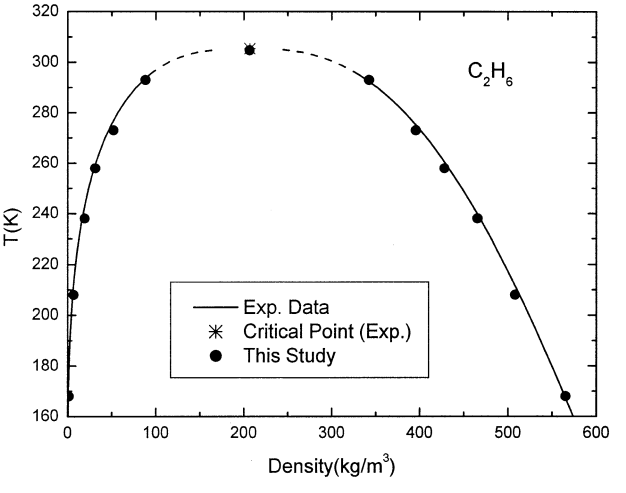

Fig. 5. Comparison of experimental liquid–vapor phase equilibria of C_2H_6 with the simulated results of this study. The solid line represents smoothed experimental data from Friend et al. (1991), and the dashed line is the extrapolation from experiment.

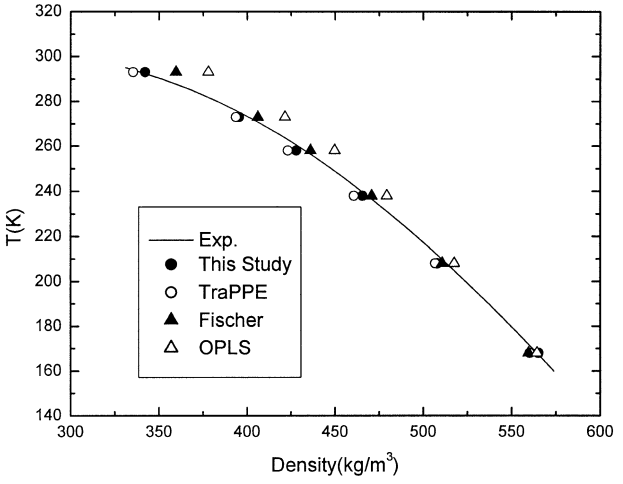

Fig. 6. Comparison of different models in the prediction of C_2H_6 liquid densities at equilibrium.

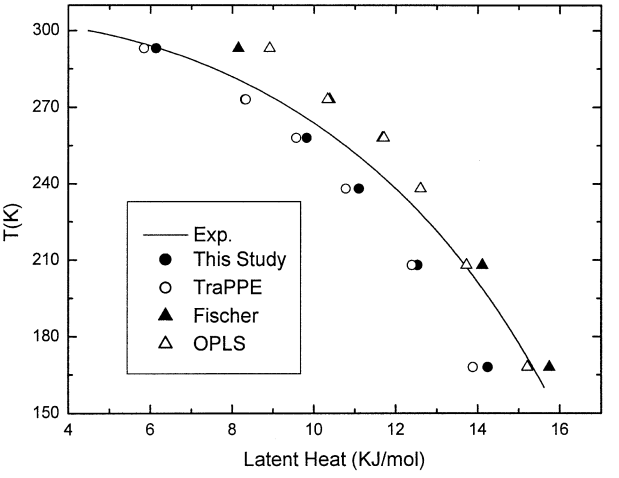

Fig. 8. The latent heat of C_2H_6: different models vs. experimental data (Friend et al., 1991).

using parameters of this study and TraPPE are very well predicted, whereas those predicted by OPLS and Fischer for C_2H_6 have a distinct deviation from experimental data (Friend et al., 1991).

It is useful to have a more detailed discussion of Figure 8. Even though the largest error is less than 10% when the parameters of TraPPE and the parameters of this study are used, the deviations are noticeable in the region of low temperatures. It is interesting that the results using OPLS and Fischer show opposite trends with temperature. The curves of different models in Figure 8 are approximately parallel with each other. It is possible that the three-parameter united-atom potential model cannot predict all of the quantities, such as the coexistence line and energy, with very good agreement with experiments simultaneously.

4.2. Mixtures

Möller et al. (1992) have presented a set of binary mixture parameters for the CH_4-C_2H_6 system from a number of complex calculations. According to their study, the mixing coefficients in Eqns. 11 and 12 are: $k_{1,ij} = 1.0009$, $k_{2,ij} = 1.0025$. In fact, with the analyses of our simulation results, coefficients with so little deviation from 1.0 almost do not affect the results because the error from the simulation noise is probably larger than this effect. In this study, both of the mixing coefficients were set to be 1.0.

The results listed in Table 6 are part of our simulated results, which cover a wide range of thermodynamic conditions. The numbers in parentheses are statistical standard deviation when each run is divided into 10 blocks discarding the preequilibrium cycles. Figure 9 displays the comparison of the simulated equilibrium composition with the corresponding experimental data (180 K from Miller et al., 1977; 210 K from Wei et al., 1995; 250 K from Davalos et al., 1976; 280 K from Gupta et al., 1980). It is satisfying that the largest deviation is less than 0.05 in mole fraction.

Figure 10 shows equilibrium compositions generated by our simulations and the predictions of the well-known EOS of Peng and Robinson (1976). Both sets of results are compared with experimental data (Gupta et al., 1980). It is found that simulations can yield a little more accurate data than PR-EOS. Figure 11 compares the simulated densities with the data extrapolated from those of Bloomer et al. (1953), showing that the equilibrium densities of the mixtures are well predicted.

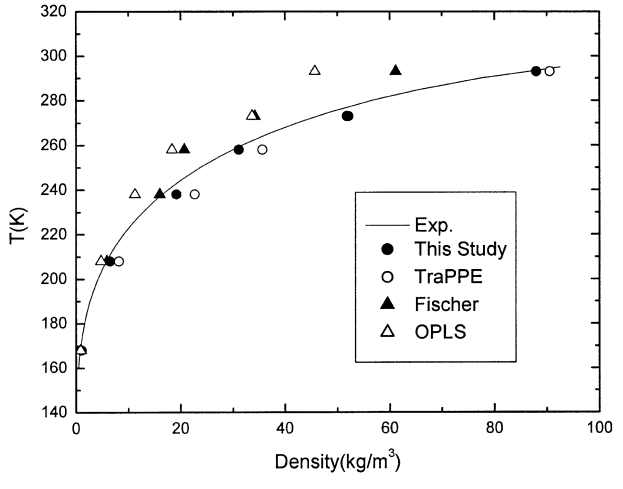

Fig. 7. Comparison of different models in the prediction of C_2H_6 vapor densities at equilibrium.

Table 5. The simulated critical points of different models.

Species	Models/Exp.	T_c(K)	ρ_c (kg/m^3)
CH_4	Exp.[a]	190.56	162.66
	This study (OPLS)	192.00	161.58
C_2H_6	Exp.[b]	305.33	206.58
	Fischer	316.42	196.58
	OPLS	325.45	196.43
	TraPPE	303.35	206.17
	This study	304.71	206.28

[a] Extrapolated from experiment by Setzmann and Wagner (1991).
[b] Extrapolated from experiment by Friend et al. (1991).

Table 6. Simulated phase equilibrium results in the system CH_4-C_2H_6.

T(K)	P(bar)	$x^1_{CH_4}$	$x^v_{CH_4}$	v^1 (cm^3/mol)	v^v (cm^3/mol)
160.0	5.98	.340(.011)	.943(.013)	49.0(.22)	2048.5(56.60)
160.0	7.93	.443(.004)	.937(.017)	48.0(.36)	1532.5(32.91)
160.0	9.93	.597(.003)	.969(.007)	47.0(.24)	1209.1(64.18)
160.0	13.38	.865(.002)	.985(.001)	47.3(.37)	805.7(36.51)
180.0	15.67	.519(.004)	.932(.013)	51.1(.19)	774.8(55.88)
180.0	21.28	.662(.004)	.968(.006)	50.6(.34)	545.6(13.12)
180.0	24.82	.834(.005)	.980(.003)	51.7(.77)	441.3(16.06)
180.0	28.28	.912(.002)	.986(.001)	53.3(.68)	368.8(17.35)
210.0	16.00	.198(.009)	.750(.010)	58.4(0.30)	955.6(30.58)
210.0	26.50	.408(.005)	.840(.019)	57.5(0.55)	513.1(18.32)
210.0	38.50	.625(.017)	.915(.010)	60.5(1.07)	326.0(19.43)
210.0	52.00	.770(.010)	.924(.015)	63.5(1.10)	200.6(30.78)
230.0	33.64	.334(.018)	.738(.013)	62.7(0.46)	426.8(27.57)
230.0	43.59	.446(.012)	.767(.019)	63.7(0.65)	294.3(15.40)
230.0	51.15	.572(.005)	.811(.013)	66.9(1.01)	241.4(11.17)
230.0	60.85	.675(.008)	.806(.039)	70.2(1.33)	137.1(30.60)
250.0	55.93	.410(.037)	.655(.017)	75.3(5.41)	226.3(12.24)
250.0	66.57	.529(.012)	.653(.021)	79.9(4.15)	146.3(16.73)
260.0	19.13	.022(.001)	.080(.002)	74.0(1.24)	894.8(5.40)
260.0	21.89	.047(.004)	.189(.006)	71.9(1.31)	777.9(23.45)
260.0	35.15	.170(.020)	.421(.013)	74.6(0.92)	461.4(10.43)
260.0	41.13	.221(.012)	.470(.014)	76.5(1.73)	376.6(10.9)
260.0	50.97	.289(.018)	.538(.030)	75.6(3.52)	283.1(9.49)
260.0	55.91	.368(.009)	.596(.030)	79.7(4.80)	249.8(32.9)
260.0	60.19	.388(.019)	.585(.025)	80.9(5.79)	206.3(19.93)
280.0	40.38	.104(.011)	.255(.009)	82.0(1.45)	404.8(17.78)
280.0	47.12	.161(.021)	.300(.010)	91.3(5.22)	307.4(15.17)
280.0	50.41	.171(.010)	.327(.011)	90.4(2.58)	287.9(17.75)
280.0	60.87	.267(.013)	.384(.014)	100.8(7.20)	199.3(8.21)
280.0	61.31	.280(.011)	.355(.021)	106.9(9.84)	181.7(9.56)

The numbers in parentheses are the uncertainties in the simulation. For example, .980(.003) means 0.980 ± 0.003.

5. CONCLUSION

The temperature scaling method combined with Gibbs Ensemble Monte Carlo was used to study the vapor–liquid equilibrium properties of CH_4 and C_2H_6. With the efficient TSGE, a new set of potential parameters for C_2H_6 was presented. Compared with previous potential parameters, the parameters of this study generally yield better results than those of Fischer et al. (1984) and OPLS (Jorgensen et al., 1984) in phase coexistence and have equivalent accuracy to TraPPE (Martin and Siepmann, 1998) in saturated liquid densities. However, this study has improved the abilities of predicting vapor properties and critical point in comparison to TraPPE. On the basis of the study of pure systems, we performed GEMC simulations for the phase equilibria of the CH_4-C_2H_6 system. Comparison of the simulated results with experimental data indicates that

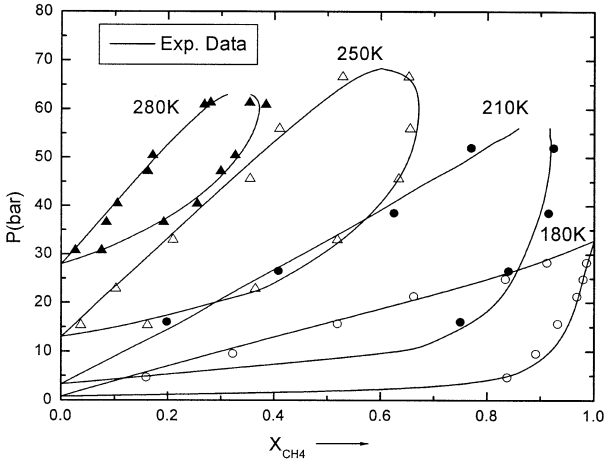

Fig. 9. Liquid–vapor phase equilibria of the mixture system CH_4-C_2H_6. Experimental data at 180 K are from Miller et al. (1977), 210 K from Wei et al. (1995), 250 K from Davalos et al. (1976), 280 K from Gupta et al. (1980).

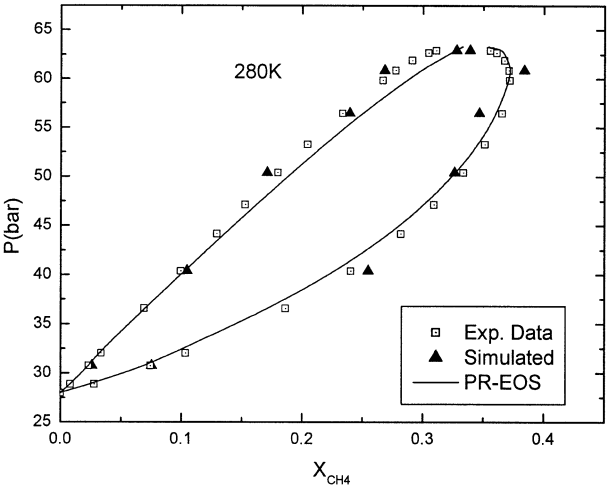

Fig. 10. Equilibrium compositions of the CH_4-C_2H_6 at 280 K. Comparison of our simulated results with the experimental data (Gupta et al., 1980) and the prediction of PR-EOS (Peng and Robinson, 1976).

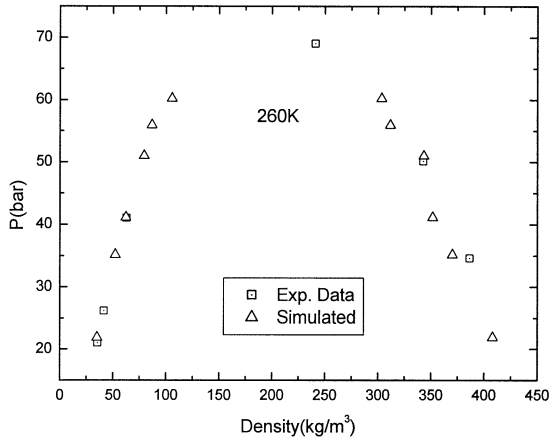

Fig. 11. Comparison of simulated mixture densities at 260 K with experimental data, which are extrapolated from those of Bloomer et al. (1953).

the equilibrium compositions and densities have been well predicted with accuracy close to experiments.

Acknowledgments—We would like to acknowledge some help from Drs. B. Chen and K. Kiyohara. We thank Dr. Mark Ghiorso, Dr. R. J. Bakker, and an anonymous reviewer for their comments and suggestions for improving the manuscript. Thanks also to Profs. Li Sitian, Xie Xinong, Zhang Wenhuai, Wang Hua, and Zhuang Xinguo for their constructive support. This work is supported by Zhenhao Duan's "Hundred Scientists Project" funds awarded by the Chinese Academy of Sciences and his outstanding young scientist funds (#49825531) awarded by the National Natural Science Foundation of P. R. China.

Associate editor: M. S. Ghiorso

REFERENCES

Allen M. P. and Tildesley D. J. (1989) *Computer Simulation of Liquids*. Oxford University Press, Oxford.

Al-Sahhaf T. A., Kidnay A. J., and Sloan E. D. (1983) Liquid-vapor equilibria in the N_2-CO_2-CH_4 system. *Ind. Eng. Chem. Fundam.* **22,** 372–380.

Anderko A. and Pitzer K. S. (1993) Equation of state representation of phase equilibria and volumetric properties of the system NaCl-H_2O above 573K. *Geochim. Cosmochim. Acta* **57,** 1657–1680.

Bloomer O. T., Gami D. C., and Parent J. D. (1953) Physical-chemical properties of CH_4-C_2H_6 mixtures. In *Institute of Gas Technology Research Bulletin*, Vol. 22, Institute of Gas Technology, Chicago.

Bodnar R. J. and Sterner S. M. (1987) Synthetic fluid inclusions. In *Hydrothermal Experimental Techniques* (eds. G. C. Ulmer and H. L. Barnes), pp. 423–457. John Wiley & Sons.

Davalos J., Anderson W. R., Phelps R. E., and Kidnay A. J. (1976) Liquid-vapor equilibria at 250.00 K for systems containing methane, ethane, and carbon dioxide. *J. Chem. Eng. Data* **21,** 81–84.

Duan Z., Moller N., and Weare J. H. (1992) Molecular dynamics simulation of PVT properties of geological fluids and a general equation of state of nonpolar and weakly polar gases up to 2000 K and 20,000 bar. *Geochim. Cosmochim. Acta* **56,** 3839–3845.

Duan Z., Moller N., and Weare J. H. (1996) A general equation of state for supercritical fluid mixtures and molecular dynamics simulation of mixture PVTX properties. *Geochim. Cosmochim. Acta* **60,** 1209–1216.

Duan Z., Moller N., and Weare J. H. (2000) Accurate prediction of the thermodynamic properties of fluids in the system H_2O-CO_2-CH_4-N_2 up to 2000 K and 100 kbar from a corresponding states/one fluid equation of state. *Geochim. Cosmochim. Acta* **64,** 1069–1075.

Fischer J., Lustig R., Breitenfelder-Manske H., and Lemming W. (1984) Influence of intermolecular potential parameters on orthobaric properties of fluids consisting of spherical and linear molecules. *Molec. Phys.* **52,** 485–497.

Friend D. G., Ingham H., and Ely J. F. (1991) Thermophysical properties of ethane. *J. Phys. Chem. Ref. Data* **20,** 275–347.

Goldstein R. H. and Reynolds T. J. (1994) Systematics of fluid inclusions in diagenetic minerals. *SEPM Short Course* **31,** 199.

Gupta M. K., Gardner G. C., Hegarty M. J., and Kidnay A. J. (1980) Liquid-vapor equilibria for the N_2 + CH_4 + C_2H_6 system from 260 to 280 K. *J. Chem. Eng. Data* **25,** 313–318.

Jansoone V. M. (1974) Dielectric properties of a model fluid with the Monte Carlo method. *Chem. Phys.* **3,** 78–86.

Jorgensen W. L., Madura J. D., and Swenson C. J. (1984) Optimized intermolecular potential functions for liquid hydrocarbons. *J. Am. Chem. Soc.* **106,** 6638–6646.

Kiyohara K., Spyriouni T., Gubbins K. E., and Panagiotopoulos A. Z. (1996) Thermodynamic Scaling Gibbs Ensemble Monte Carlo: A new method for determination of phase coexistence properties of fluid. *Molec. Phys.* **89,** 965–974.

Kofke D. A. (1993a) Direct evaluation of phase coexistence by molecular simulation via integration along the saturation line. *J. Chem. Phys.* **98,** 4149–4162.

Kofke D. A. (1993b) Gibbs-Duhem integration: A new method for direct evaluation of phase coexistence by molecular simulation. *Molec. Phys.* **78,** 1331–1336.

Kriebel C., Müller A., Winkelmann J., and Fischer J. (1995) Vapour liquid equilibria of two-centre Lennard-Jones fluids from the NpT plus test particle method. *Molec. Phys.* **84,** 381–394.

Litvinovsky B. A. (1993) CO_2-H_2O fluids in lower and middle crust: Role in magma generation and metamorphism. *Daklady Akademii Nauk.* **332,** 75–78.

Martin M. G. and Siepmann J. I. (1998) Transferable potentials for phase equilibria. 1. United-Atom description of n-Alkanes. *J. Phys. Chem. B* **102,** 2569–2577.

Miller R. C., Kidnay A. J., and Hiza M. J. (1977) Liquid + vapor equilibria in methane + ethene from 150.00 to 190.00 K. *J. Chem. Thermodynamics* **9,** 167–178.

Möller D., Oprzynski J., Müller A., and Fischer J. (1992) Prediction of thermodynamic properties of fluid mixtures by molecular dynamics simulations: Methane-ethane. *Molec. Phys.* **75,** 363–378.

Nicholson K. (1993) *Geothermal Fluids: Chemistry and Exploration Techniques*. Springer Verlag, Berlin.

Panagiotopoulos A. Z. (1987) Direct determination of phase coexistence properties of fluids using Monte Carlo simulation in a new ensemble. *Molec. Phys.* **61,** 813–826.

Panagiotopoulos A. Z., Quirke N., Stapleton M., and Tildesley D. J. (1988) Phase equilibria by simulation in the Gibbs Ensemble: Alternative derivation, generalization and application to mixture and membrane equilibria. *Molec. Phys.* **63,** 527–545.

Panagiotopoulos A. Z., Wong V., and Floriano M. A. (1998) Phase equilibria of lattice polymers from Histogram Reweighting Monte Carlo simulations. *Macromolecules* **31,** 912–918.

Panagiotopoulos A. Z. (2000) Monte Carlo methods for phase equilibria of fluids. *J. Phys. Condens. Matter* **12,** R25–R52.

Peng D. Y. and Robinson D. B. (1976) A new two constants equation of state. *Ind. Eng. Chem. Fundam.* **15,** 59–64.

Potoff J. J. and Panagiotopoulos A. Z. (1998) Critical point and phase behavior of the pure fluids and a Lennard-Jones mixture. *J. Chem. Phys.* **109,** 10914–10920.

Roedder E. (1984) Fluid inclusions. In *Reviews in Mineralogy*, Vol. 12, Mineralogical Society of America, Washington, D. C.

Setzmann U. and Wagner W. (1991) A new equation of state and tables of thermodynamic properties for methane covering the range from the melting line to 625 K at pressures up to 1000 MPa. *J. Phys. Chem. Ref. Data* **20,** 1061–1151.

Seward T. M. and Barnes H. L. (1997) Metal transport by hydrothermal ore fluids. In *Geochemistry of Geothermal Ore Deposits* (ed. H. L. Barnes), pp. 435–486. John Wiley & Sons.

Valleau J. P. (1993) Density-Scaling Monte Carlo study of subcritical Lennard-Jonesium. *J. Chem. Phys.* **99,** 4718–4728.

Vrabec J. and Fischer J. (1995) Vapour liquid equilibria of mixtures from the NpT+test particle method. *Molec. Phys.* **85,** 781–792.

Wei W., Brown T. S., Kidnay A. J., and Sloan E. D. (1995) Vapor + liquid equilibria for the ternary system methane + ethane + carbon dioxide at 230 K and its constituent binaries at temperatures from 207 to 270K. *J. Chem. Eng. Data* **40,** 726–732.